The Journal of Experimental Biology 205, 1293–1303 (2002)
Printed in Great Britain © The Company of Biologists Limited 2002
JEB3842

Temperature adaptation in *Gillichthys* (Teleost: Gobiidae) A_4-lactate dehydrogenases: identical primary structures produce subtly different conformations

Peter A. Fields[1,*], Yong-Sung Kim[2], John F. Carpenter[2] and George N. Somero[1]

[1]*Hopkins Marine Station, Biological Sciences Department, Stanford University, Pacific Grove, CA 93950, USA* and [2]*School of Pharmacy, Department of Pharmaceutical Sciences, University of Colorado Health Sciences Center, Denver, CO 80262, USA*

*Author for correspondence and present address: Department of Biology, Franklin and Marshall College, PO Box 3003, Lancaster, PA 17604, USA (e-mail: p_fields@fandm.edu)

Accepted 8 February 2002

Summary

Alternative conformations of proteins underlie a variety of biological phenomena, from prion proteins that cause spongiform encephalopathies to membrane channel proteins whose conformational changes admit or exclude specific ions. In this paper, we argue that conformational differences within globular 'housekeeping' enzymes may allow rapid adaptation to novel environments. Muscle-type lactate dehydrogenases (A_4-LDHs) from the gobies *Gillichthys seta* and *G. mirabilis* have identical amino acid sequences but show potentially adaptive differences in substrate affinity (apparent Michaelis constants for pyruvate, K_m^{PYR}) as well as differences in thermal stability. We examined the A_4-LDH of each species using fluorescence spectroscopy, near- and far-ultraviolet circular dichroism (CD) spectroscopy and hydrogen/deuterium exchange (H/D) Fourier-transform infrared spectroscopy to determine whether structural differences were apparent, the extent to which structural differences could be related to differences in conformational flexibility and whether specific changes in secondary or tertiary structure could be defined. The fluorescence spectra and far-ultraviolet CD spectra of the A_4-LDH from the two species were indistinguishable, suggesting that the two conformations are very similar in secondary and tertiary structure. Apparent melting temperatures (T_m) followed by fluorescence and CD spectroscopy confirmed that the *G. mirabilis* A_4-LDH is more thermally stable than the *G. seta* form. H/D exchange kinetics of *Gillichthys* A_4-LDH was described using double-exponential regression; at 20 °C, *G. seta* A_4-LDH has a higher exchange constant, indicating a more flexible and open structure. At 40 °C, the difference in H/D exchange constants disappears. Second-derivative analysis of H/D exchange infrared spectra indicates that α-helical, but not β-sheet structure, differs in conformational flexibility between the two forms. Second-derivative ultraviolet spectra indicate that at least one of the five tyrosyl residues in the *Gillichthys* LDH-A monomer is located in a more hydrophobic environment in the *G. mirabilis* form. Homology models of A_4-LDH indicate that Tyr246 is the most likely candidate to experience a modified environment because it is involved in subunit contacts within the homotetramer and sits in a hinge between a static α-helix and one involved in catalytic conformational changes. Subtle differences in conformation around this residue probably play a role both in altered flexibility and in the potentially adaptive differences in kinetics between the two A_4-LDH forms.

Key words: A_4-LDH, alternative conformation, conformational flexibility, *Gillichthys mirabilis*, *Gillichthys seta*, temperature adaptation, lactate dehydrogenase.

Introduction

Interest in polypeptides that can adopt multiple conformations has exploded in recent years as a result of the discovery of pathogenic prion proteins (PrPs) in mammals (Cohen and Prusiner, 1998) and the non-pathogenic Sup35 prion in yeast (Patino et al., 1996). These recent findings have been presaged by studies extending back over three decades showing that more subtle conformational changes in enzymes with known function are relatively common. For example, Marangos and Constantides (1974) presented evidence that glyceraldehyde-3-phosphate dehydrogenase from flounder (*Pseudopleuronectes americanus*) liver exists in multiple conformations *in vivo*, apparently because of alternative multimeric forms composed of the same subunit type. Rabbit muscle adenylate cyclase has been shown to exist in at least two native forms (Zhang et al., 1998), differentially susceptible to urea denaturation. Chazin et al. (1989) observed multiple

conformations of calbindin D_{9k} and used ^1H nuclear magnetic resonance to prove that the source of conformational variability is *cis–trans* isomerization of a single proline residue. In *Drosophila melanogaster*, alcohol dehydrogenase, a protein coded by a single genetic locus, has also been shown to exist in multiple electrophoretically separable forms with different thermal stabilities (Jacobson et al., 1970), which are interconvertable. Xue and Yeung (1995) were able to observe single lactate dehydrogenase (LDH) molecules using capillary spectrophotometry, and showed that 'homogeneous' preparations were composed of discrete populations with significant differences (up to fourfold) in reactivity, which the authors argued were best explained by differing arrangements of the four identical subunits.

These studies reveal that single polypeptides with multiple three-dimensional conformations are numerous. Few studies, however, have shown instances in which such modifications of protein structure might be adaptive, i.e. where the alternative conformers function optimally in different environments and are produced differentially as environmental parameters dictate. Somero (1969) showed that pyruvate kinase from the Alaskan king crab (*Paralithodes camtschatica*) occurs as both a 'warm' and 'cold' variant, depending on measurement temperature, and that these variants have different apparent Michaelis constants for the substrate phosphoenolpyruvate. Similarly, Ozernyuk et al. (1994) found that the muscle-type LDH (A_4-LDH) of the loach (*Misgurnus fossilis*) occurs in two forms with differing kinetics depending on season and that both could be converted to a single form with intermediate characteristics by brief exposure to 3 mol l^{-1} urea.

A recent study by Fields and Somero (1997) showed that the A_4-LDHs (EC 1.1.1.27; NAD^+:lactate oxidoreductase) of two closely related species of goby, *Gillichthys mirabilis* and *G. seta*, have identical primary sequences despite four synonymous differences in the coding regions of their mRNAs. However, these orthologs have different substrate affinities, as measured by apparent Michaelis constants for the substrate pyruvate (K_m^{PYR}), as well as different thermal stabilities. The two species live in disparate habitats: *G. seta* occupies the high rocky intertidal zone in the northern Gulf of California (latitude approximately 31°N) and experiences broader and warmer temperatures (approximately 5–41 °C) than its congener *G. mirabilis* (approximately 9–30 °C), which lives in sloughs and estuaries from the Gulf of California north along the west coast of North America to Tomales Bay (latitude 38.16°N) (Miller and Lea, 1972).

The K_m^{PYR} values measured for the A_4-LDH orthologs of the two species reflect these environmental differences: at any measurement temperature, the A_4-LDH of *G. seta* has a lower K_m^{PYR} value than does the A_4-LDH of *G. mirabilis*, indicating greater substrate affinity. Further, *G. seta* A_4-LDH K_m^{PYR} is less affected by temperature change within the range 10–40 °C than is the *G. mirabilis* form. The two orthologs were shown to have an identical mass using ion-spray mass spectrometry (Fields and Somero, 1997), thus discounting the possibility of post-translational covalent modification. Moreover, on the basis of the work of Ozernyuk et al. (1994) described above, gentle denaturation with urea (3 mol l^{-1} for 15 min) resulted in an increase in the K_m^{PYR} of *G. seta* A_4-LDH, rendering it indistinguishable from that of *G. mirabilis* A_4-LDH. We concluded, therefore, that the differences in kinetics between the two native forms must be due to modifications in tertiary or quarternary interactions unique to the ortholog of each species. Interestingly, maintaining populations of the two species for extended periods at the same temperature (>3 months at 15 °C) (Fields and Somero, 1997) did not change the K_m^{PYR} or thermal stability of either A_4-LDH ortholog. This suggests that the conformational differences between the orthologs is not a result of temperature acclimation and is, instead, a permanent phenotypic characteristic.

To describe better the conformational differences between the *G. mirabilis* and *G. seta* orthologs that may underlie the measured differences in substrate affinity and thermal stability, we have examined each using circular dichroism (CD) and fluorescence spectroscopy, which provide measures of secondary and tertiary protein structure, respectively. We have also used hydrogen/deuterium exchange monitored by Fourier-transform infrared spectroscopy (H/D-FTIR), which measures the rate at which amide hydrogens buried within the native fold of the protein are transiently exposed to the solvent medium, to examine in greater detail the differences in molecular flexibility that might explain the changes we found in substrate affinity and thermal stability between the two orthologs. We performed CD and H/D-FTIR spectroscopy at 20 and 40 °C, temperatures within the range that *G. seta* experiences but extending above those that *G. mirabilis* experiences, to determine how temperature change affects the structure of A_4-LDH in these species.

In this paper, we show (i) that the orthologs have identical fluorescence and far-ultraviolet CD spectra, indicating that their secondary and tertiary structures are identical; (ii) that *G. seta* A_4-LDH has a faster H/D exchange rate than the *G. mirabilis* form at 20 °C, suggesting greater conformational flexibility in the former; (iii) that differences in conformational flexibility can be associated with α-helical, but not β-sheet, structure and (iv) that, on the basis of a comparison of second-derivative ultraviolet spectra, at least one of the five tyrosyl residues, but none of the six tryptophyl residues, in the *G. mirabilis* LDH-A monomer is in a more hydrophobic environment than the corresponding residue in the *G. seta* ortholog. Using this evidence, we argue that the conformational differences between the forms responsible for the potentially adaptive differences in K_m^{PYR} probably occur in a small region of the molecule bounding helix α1G–α2G, a structure whose mobility is closely tied to the catalytic rate and substrate affinity of A_4-LDH (Fields and Somero, 1998; Dunn et al., 1991).

Materials and methods

Experimental animals

Gillichthys mirabilis were caught using baited minnow traps in a brackish slough 20 km north of Monterey, California,

USA, during May–July 2000. They were kept in aerated ambient-temperature (approximately 15 °C) aquaria at Hopkins Marine Station, Pacific Grove, California, USA, until they were used in experiments. *Gillichthys seta* were caught by hand on a rocky beach near Puerto Peñasco, Mexico, on the eastern shore of the Gulf of California during Autumn 1999. Individuals were transported back to Hopkins Marine Station and kept in aerated ambient-temperature aquaria until they were used in experiments.

Purification of A4-LDH

White epaxial muscle was dissected from freshly killed individuals; contamination from the skin and viscera was minimized to avoid contamination by heart-type (B_4) LDH. Muscle tissue was homogenized and centrifuged, and A_4-LDH was purified from the supernatant using oxamate-affinity chromatography (Yancey and Somero, 1978), as described previously (Fields and Somero, 1997). Lactate dehydrogenase binds tightly to oxamate in the presence of NADH, so an extended wash with NADH-containing buffer ensured the removal of other proteins together with any small molecules that might have been loosely bound to LDH. The purity of the A_4-LDH was confirmed using sodium dodecyl sulfate polyacrylamide gel electrophoresis (SDS–PAGE) followed by silver staining; only one protein band was seen for each species of fish.

An initial goal of the study was to compare the structures of the wild-type A_4-LDHs with those of the urea-denatured A_4-LDHs, which showed identical K_m^{PYR} values in the two species (Fields and Somero, 1997). We were unable, however, to purify enough urea-treated A_4-LDH for the structural studies described below because of irreversible loss of activity of the enzyme during the brief denaturation process. Thus, we describe only a comparison of the wild-type A_4-LDHs from the two congeners.

Samples of purified A_4-LDH were precipitated and stored in 90 % ammonium sulfate until analyses were performed. The ammonium sulfate was removed, and the samples were concentrated by repeated washing with 10 mmol l^{-1} potassium phosphate buffer (pH 7.0) in a Centricon-30 (Amicon, Beverly, MA, USA) centrifugal separator.

Fluorescence spectroscopy

Intrinsic tryptophan fluorescence spectra for A_4-LDH from both fish species were measured from 310 to 400 nm in an Aviv ATF 105 spectrofluorometer using an excitation wavelength of 295 nm. A_4-LDH concentration was 20 μg ml^{-1} in 10 mmol l^{-1} potassium phosphate buffer (pH 7.0), and cuvette temperature was maintained at 20 °C.

To monitor thermal unfolding of the A_4-LDH orthologs, fluorescence intensity was monitored at 347 nm as cuvette temperature was stepped from 20 to 85 °C in increments of 0.5 °C. At each temperature, samples were equilibrated for 30 s, followed by signal-averaging for 10 s. The resultant data were analyzed by complex sigmoid, non-linear least-squares fitting to obtain the fraction of protein molecules unfolded at each temperature and the apparent midpoint of the native→denatured transition region (Pace, 1986; Kim et al., 2000). The latter datum is used as an estimate of the apparent melting temperature, T_m, which is an indicator of global protein stability.

Circular dichroism spectroscopy

All CD spectra were produced using an AVIV 60DS spectropolarimeter. Far-ultraviolet spectra of *G. mirabilis* and *G. seta* A_4-LDHs were collected from 190 to 260 nm using a 0.1 cm path-length quartz cuvette; buffer spectra were also collected and subtracted from each protein spectrum. The protein concentration used for far-ultraviolet spectroscopy was approximately 0.1 mg ml^{-1}. Ellipticity data thus obtained were converted to mean residue ellipticity, Θ_{MRW}, using the equation:

$$\Theta_{MRW} = \Theta M_o / 10cl ,$$

where Θ is ellipticity in millidegrees, M_o is the mean residue molecular mass [the molecular mass of *Gillichthys* A_4-LDH, 36 165 Da (Fields and Somero, 1997), divided by the number of residues (331)], c is the protein concentration (in mg ml^{-1}) and l is the path length of the cell (in cm).

Thermal denaturation profiles were obtained by monitoring ellipticity at 222 nm while increasing cuvette temperature in increments of 1 °C from 25 to 85 °C, equilibrating at each temperature for 12 s and signal-averaging for 5 s. Values of T_m for each sample were calculated using the method of Pace (1986) and Kim et al. (2000) described above.

In the near-ultraviolet CD experiments, absorbance spectra were collected between 270 and 300 nm, buffer absorbance was subtracted and values were converted to mean residue ellipticity as described above. Second-derivative ultraviolet spectra were calculated using Grams 386 software (Galactic Industries); such second-derivative spectra are sensitive to the global environment of aromatic amino acids and are especially useful in reporting changes in the hydrophobicity of the environment surrounding Tyr residues. According to the method of Servillo et al. (1982), the ratio $r=a/b$, where a is the difference between the minimum of the second-derivative spectrum at approximately 283 nm and the maximum at approximately 287 nm (Tyr signal) and b is the difference between the minimum at approximately 291 nm and the maximum at approximately 296 nm (Trp signal) (see Results), is indicative of the relative number of Tyr and Trp residues as well as the hydrophobicity of the Tyr environment. Values of r were calculated for each form of A_4-LDH at 20, 30 and 40 °C.

Although r should be independent of protein concentration (Ragone et al., 1984), we performed the following analysis to ensure that minor differences in protein concentration did not affect the results of the second-derivative ultraviolet study. The spectra were eight-times-interpolated and area-normalized between 250 and 310 nm to correct for potential differences in protein concentration. A new second-derivative spectrum was calculated from each of these area-normalized ultraviolet spectra and compared with the corresponding original second-

derivative spectrum. The differences between second-derivative spectra of A_4-LDH within each species were negligible compared with the differences found between the A_4-LDH orthologs.

Hydrogen/deuterium exchange

All H/D exchange assays were performed in a Bomem MB-series FTIR spectrometer with a temperature-controlled cell holder. A_4-LDH samples were diluted to a concentration of approximately 0.75 mg ml^{-1} in aqueous or 75 % D_2O buffer (10 mmol l^{-1} potassium phosphate, pH 7.0) and were immediately injected into a CaF_2 cell with a 25 μm Teflon spacer. Spectra were collected 2, 7, 12, 17, 25, 40 and 60 min after injection into the sample cell and every 30 min thereafter up to 360 min for 20 °C assays and up to 300 min for 40 °C assays. Reference spectra were collected with buffer only in the sample cell before each experimental assay. The spectra of liquid and gaseous water were subtracted from each sample spectrum according to the method of Dong et al. (1992), and the resulting spectrum was smoothed with a seven-point Savitsky–Golay function as implemented by the Grams 386 software.

The ratio of the amide II peak (centered at approximately 1550 cm^{-1}) to the amide I peak (centered at approximately 1655 cm^{-1}) for each spectrum was determined, and the change in this ratio with time exposed to D_2O was used as an indication of the rate of exchange of internal amide hydrogens with solvent deuterons. The resultant decay plots were fitted with a double-exponential equation to produce a smoothed curve, and the exponents of these curves were taken as the time constants of H/D exchange in subpopulations of amide hydrogens.

To determine H/D exchange rates in specific secondary structures, second-derivative spectra were calculated from the aqueous spectrum and the H/D spectra over time for both A_4-LDH forms at 20 and 40 °C. Each second-derivative spectrum was baseline-corrected (Dong and Caughey, 1994) and area-normalized under the amide I region (Kendrick et al., 1996, 1997). Because peaks in the second-derivative infrared spectrum within the amide I region correspond to specific secondary structures (i.e. α-helix, β-sheet, turn), this analysis allowed H/D exchange in distinct areas of the A_4-LDH molecule to be compared.

Homology modeling

To examine the positions of Tyr residues within the three-dimensional fold of *Gillichthys* A_4-LDH, we used the SWISS-MODEL program (Guex and Peitsch, 1997) to create a structural homology model. We overlaid the primary structure of the *Gillichthys* protein on two templates consisting of dogfish A_4-LDH (Protein Data Bank code 1LDM) (Abad-Zapatero et al., 1987) and pig A_4-LDH (9LDT) (Dunn et al., 1991). An alignment of the three A_4-LDH sequences is available from the authors upon request. The crystallographically-derived three-dimensional conformations of the pig and dogfish orthologs are very similar in secondary and tertiary structure and, because their phylogenetic divergence precedes that of pig and teleost, we are confident that they are appropriate templates for the development of the *Gillichthys* A_4-LDH model. The resulting coordinate file was used to visualize the positions of the residues of interest in the molecule, their exposure to solvent and their role in inter-subunit interactions.

Results

Fluorescence spectra

Fig. 1A shows Trp fluorescence emission spectra of *G. mirabilis* and *G. seta* A_4-LDH at 20 °C. The wavelength of maximum emission intensity, the peak width at half height and the skewness of the peak are indistinguishable between the spectra. These similarities in the Trp fluorescence of the two A_4-LDHs indicate that each of the six Trp residues is found in comparable environments within the two forms. Fig. 1B shows the pattern of thermal unfolding of each A_4-LDH form as followed by Trp fluorescence at 347 nm. Unfolding resulted in visible aggregation of protein in the cuvette, indicating that the process was not reversible. However, we argue that this does not affect our conclusions because protein concentrations were the same for each assay and we are interested in relative, rather than absolute, protein stability. It is clear that, despite the similarity between the forms shown in Fig. 1A, *G. seta* A_4-LDH unfolds at a lower temperature than does *G. mirabilis* A_4-LDH. The midpoints of the thermal unfolding transition regions, T_m, derived from this analysis are 55.5±0.1 °C for *G. seta* A_4-LDH and 58.4±0.1 °C (apparent midpoint of transition ± S.E.M.) for the *G. mirabilis* form. These results agree with earlier work that showed a lower thermal stability for *G. seta* A_4-LDH than for *G. mirabilis* A_4-LDH (Fields and Somero, 1997).

Circular dichroism spectroscopy

Fig. 2A shows far ultraviolet CD spectra for *G. mirabilis* and *G. seta* A_4-LDHs at 20 and 40 °C. At both temperatures, the spectra are indistinguishable. This indicates that the secondary structures of the two A_4-LDH forms are similar and that they maintain their similarity at temperatures at which differences in conformational flexibility are significant (see H/D exchange below). Coupled with the Trp fluorescence data described above, these findings suggest that the A_4-LDHs of the two *Gillichthys* species possess secondary and tertiary structures that are identical within the sensitivities of the two techniques.

Thermal denaturation profiles were followed with far-ultraviolet CD at 222 nm (Fig. 2B) and produced results similar to the thermal denaturation assays followed by Trp fluorescence (Fig. 1B). A_4-LDH from *G. mirabilis* had an apparent T_m of 60.2±0.1 °C and the *G. seta* form had an apparent T_m of 58.4±0.1 °C. These values are higher than the T_m values derived by Trp fluorescence. This difference probably reflects the loss of secondary structure, which CD monitors, at temperatures higher than the quarternary and tertiary structure to which Trp fluorescence is sensitive. Nevertheless, both methods produce the same result: *G.*

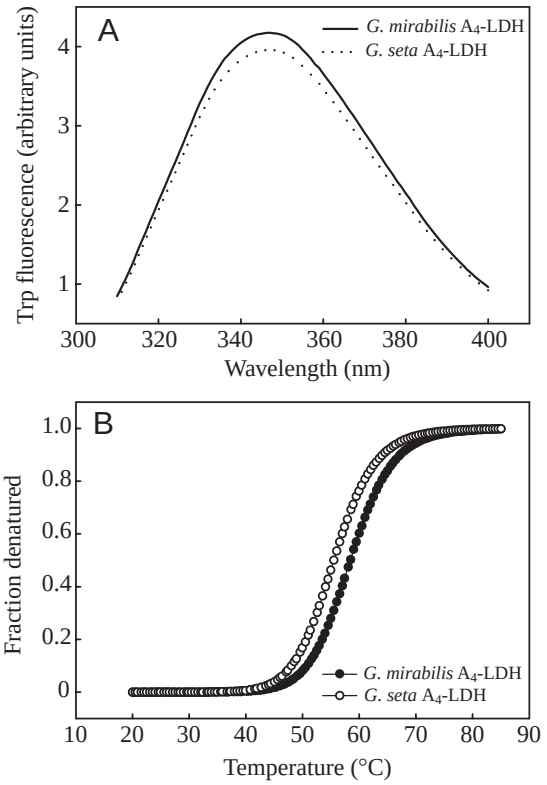

Fig. 1. (A) Buffer-corrected tryptophan fluorescence spectra of *Gillichthys mirabilis* and *G. seta* muscle-type lactate dehydrogenases (A_4-LDHs) at 20 °C. Excitation wavelength was 295 nm. (B) Thermal denaturation profiles of the A_4-LDH forms monitored using tryptophan fluorescence (excitation wavelength 295 nm, emission wavelength 377 nm). Curves were fitted to the data as described in the text. *Gillichthys mirabilis* A_4-LDH T_m=58.4±0.1 °C and *G. seta* A_4-LDH T_m=55.5±0.1 °C.

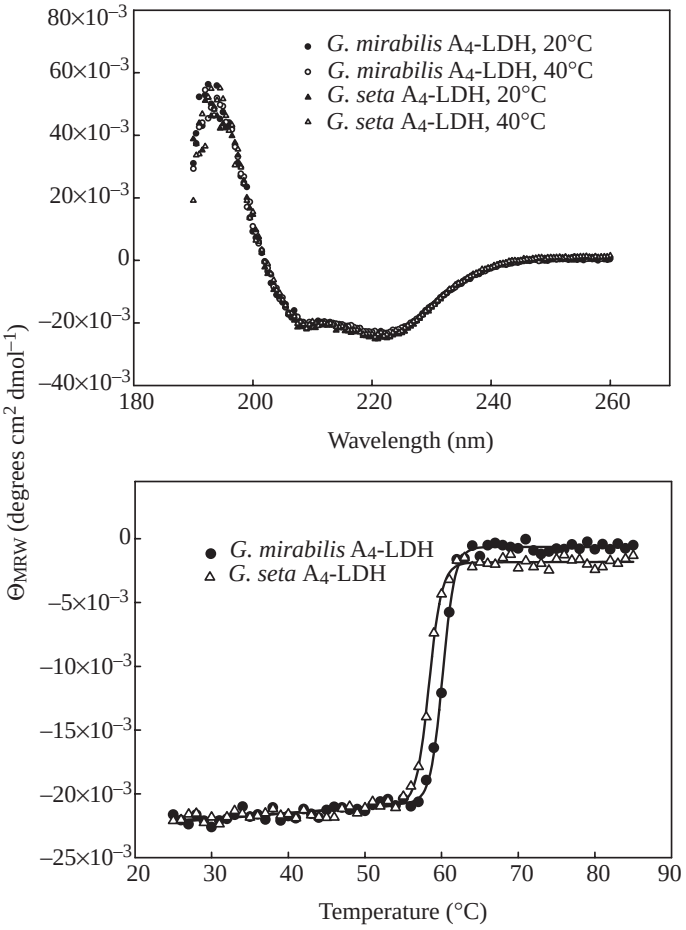

Fig. 2. (A) Buffer-corrected far-ultraviolet circular dichroism (CD) spectra of *Gillichthys mirabilis* and *G. seta* muscle-type lactate dehydrogenases (A_4-LDHs) at 20 and 40 °C. (B) Thermal denaturation profiles of the A_4-LDH forms monitored using CD spectroscopy; absorbance was measured at 222 nm. Curves were fitted as described in the text; *G. mirabilis* A_4-LDH T_m=60.2±0.1 °C and *G. seta* A_4-LDH T_m=58.4±0.1 °C). Θ_{MRW}, residue ellipticity.

mirabilis A_4-LDH maintains its native structure to temperatures higher than does *G. seta* A_4-LDH.

Near-ultraviolet CD spectra for the two A_4-LDH forms at 20 °C are shown in Fig. 3A. Near-ultraviolet spectra include absorbance signals from Trp and Tyr residues at approximately 295 and approximately 275 nm, respectively, and the subtraction spectrum (*G. mirabilis* minus *G. seta*) indicates that the Trp absorbance does not differ significantly between the two forms but that the Tyr absorbance is higher for *G. seta* A_4-LDH. These results suggest that the environments in which the six Trp residues are found are similar in the two A_4-LDHs, which is consistent with the Trp fluorescence data (Fig. 1A), but that at least one of the five Tyr residues occupies a different environment between the two forms.

Fig. 3B shows the second-derivative near-ultraviolet absorbance spectra of the two *Gillichthys* A_4-LDHs at 20 °C. Second-derivative ultraviolet spectra are useful for resolving overlapping peaks, such as the peaks caused by Trp and Tyr absorbance at approximately 295 and approximately 275 nm. The ratio *r* between values *a* (the difference between the trough at approximately 283 and the peak at approximately 287 nm) and *b* (the difference between the trough at approximately 291 and the peak at approximately 296 nm) provides information regarding both the relative number of Tyr and Trp residues in the protein and the environment in which the Tyr residues occur (Ragone et al., 1984). For *G. mirabilis* A_4-LDH at 20 °C, *r*=0.51; for the *G. seta* form, *r*=0.71. Because the numbers and positions of Tyr and Trp residues are identical between the two forms, the difference in *r* values indicates that at least one Tyr in the *G. mirabilis* LDH-A monomer is in a more hydrophobic environment than the corresponding residue in the *G. seta* ortholog. Values of *r* at 30 and 40 °C for *G. mirabilis* A_4-LDH are 0.49 and 0.43, and for the *G. seta* form are 0.66 and 0.61, respectively. The reduction in *r* with increasing temperature indicates that the environment around the variable Tyr residue(s) is becoming more hydrophobic, but the effect is comparable between species. Because thermal denaturation monitored by Trp fluorescence (Fig. 1B) or CD spectroscopy (Fig. 2B) shows that both A_4-LDH forms remain in the native state above 40 °C, and both forms of A_4-LDH are active

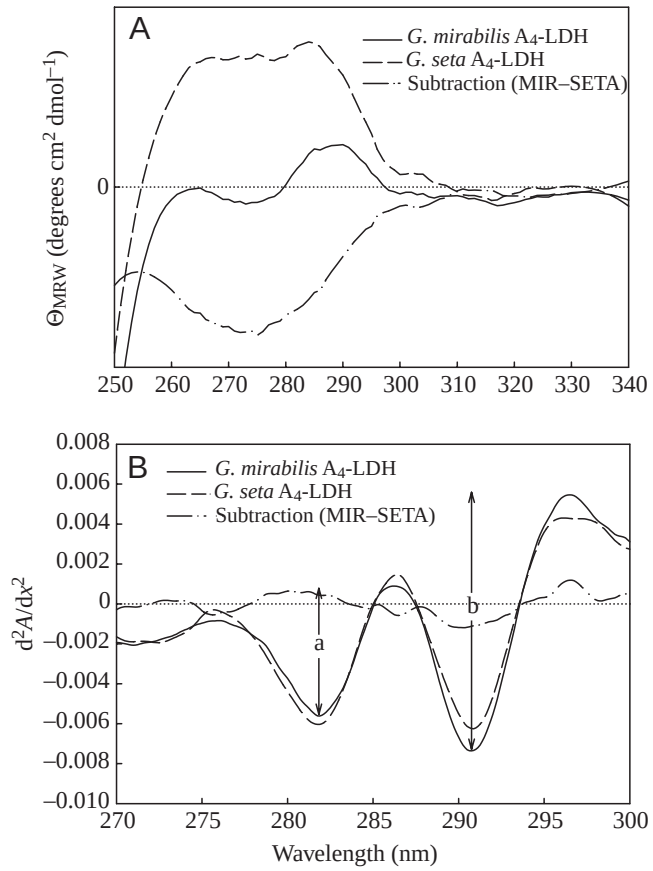

Fig. 3. (A) Near-ultraviolet circular dichroism (CD) spectra of *Gillichthys mirabilis* and *G. seta* muscle-type lactate dehydrogenases (A_4-LDHs) at 20 °C, and the subtraction spectrum (*G. mirabilis* minus *G. seta*; MIR minus SETA). (B) Second-derivative absorbance spectra of the two forms at 20 °C and the subtraction spectrum. The peak-to-trough distances, *a* and *b*, used to calculate the ratio *r* are illustrated. Note the difference in *x*-axis range between the two panels. Mir, to be defined; SETA, to be defined; Θ_{MRW}, residue ellipticity; d^2A/dx^2, second derivative of the spectrum.

at 40 °C (Fields and Somero, 1997), this increase in hydrophobicity cannot be due to denaturation and aggregation. Instead, we speculate that the source of increased hydrophobicity at higher temperatures may be either the formation of soluble oligomers or a subtle rearrangement of subunits within the A_4-LDH tetramer. Further research is necessary to determine the underlying cause of the changes in the Tyr environment with increasing temperature.

Hydrogen/deuterium exchange

When a protein is placed in deuterated water, amide hydrogens on the exterior of the molecule exchange with solvent deuterons almost instantaneously. Those amide hydrogens that are protected from solvent exposure by their location in the interior of the protein will exchange only when they too become exposed to solvent. Because the conditions of our H/D exchange experiments, pH 7.0 and 20 or 40 °C, maintain the native state of the protein (i.e. there is no thermal or acid denaturation), exchange of internal amide hydrogens occurs predominantly through small-scale (local) fluctuations rather than through partial or global unfolding (Kendrick et al., 1997; Miller and Dill, 1995). Different groups of amide hydrogens within the protein are exposed at different rates, depending on the type, rigidity and location of the structures to which they belong (Hvidt and Nielsen 1966). It is the exchange of these internal amide hydrogens that we have measured using H/D-FTIR spectroscopy. The rates at which these amide hydrogens exchange under different experimental conditions can then be correlated with differences in flexibility between the two A_4-LDH forms or with flexibility changes within one form at two different temperatures.

Infrared spectroscopy is used to monitor H/D exchange by following the ratio of the amide II (approximately 1550 cm^{-1}) peak to the amide I (approximately 1650 cm^{-1}) peak, which decreases during H/D exchange as the amide II peak is replaced by a red-shifted amide II′ peak (approximately 1450 cm^{-1}) (Dong et al., 1996). Fig. 4 shows changes in the amide II/amide I ratio for A_4-LDH from *G. mirabilis* and *G. seta* at both 20 and 40 °C. Double-exponential decay curves were fitted to the data using Sigmaplot non-linear regression software (Jandel Scientific, San Rafael, CA, USA), and rate constants were derived from these regressions.

It is clear from an examination of Fig. 4 that there are two separate exchange rate constants for each of the A_4-LDHs at the two test temperatures; these rate constants represent the major populations of amide hydrogens exchanging during the time course of the experiment (360 min at 20 °C, 300 min at 40 °C). At 20 °C, the fast exchange constant for *G. seta* A_4-LDH is greater than that for *G. mirabilis* A_4-LDH ($4.00e^{-2}$ min^{-1} *versus* $3.28e^{-2}$ min^{-1}), but the slow exchange constants are similar ($1.82e^{-4}$ min^{-1} *versus* $1.95e^{-4}$ min^{-1}). At 40 °C, all exchange rates have increased, which is expected given the greater conformational flexibility of proteins at

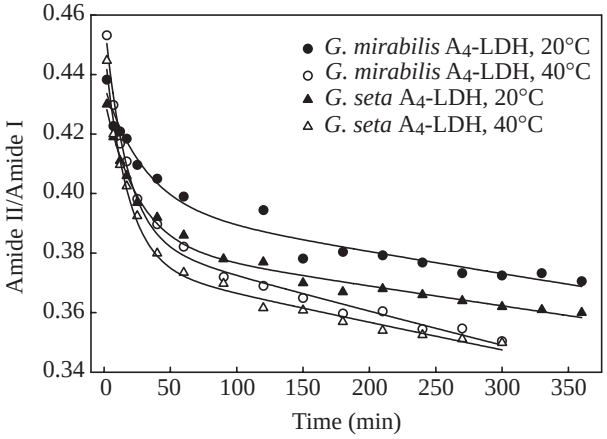

Fig. 4. Change in the ratio of amide II to amide I peaks over time during hydrogen/deuterium exchange monitored by infrared spectroscopy. Symbols represent data collected, lines represent the best fit of a double-exponential decay to each experiment, as described in the text.

higher temperature. However, there is no longer a difference in the fast exchange constants between the two A_4-LDHs ($5.93e^{-2}\,min^{-1}$ *versus* $6.00e^{-2}\,min^{-1}$ for *G. seta* and *G. mirabilis* A_4-LDHs, respectively); at 40 °C, the slow exchange constant of *G. mirabilis* A_4-LDH is higher than that of *G. seta* ($3.22e^{-4}\,min^{-1}$ *versus* $2.64e^{-4}\,min^{-1}$).

From these data, we conclude that at 20 °C the most rapidly exchanging subpopulation of amide hydrogens is replaced more quickly in *G. seta* A_4-LDH than it is in *G. mirabilis* A_4-LDH. As temperature is raised to 40 °C, this difference is lost. These results suggest that at 20 °C the outermost secondary structural components of the *G. seta* A_4-LDH molecule are more flexible (and more often transiently exposed to the deuterated solvent) than the same regions in the *G. mirabilis* molecule. However, the *G. mirabilis* form shows a greater increase in conformational flexibility with temperature, so that at 40 °C the difference in rapid H/D exchange between the two forms has been lost.

In addition, Fig. 4 shows that the rate of change of the amide II/amide I ratio of *G. mirabilis* A_4-LDH shifts from being dominated by the fast exchange constant to being dominated by the slow exchange constant at a higher amide II/amide I value than does that of *G. seta* A_4-LDH. That is, in *G. mirabilis* A_4-LDH, the slope of the curve of amide II/amide I *versus* time 'flattens out' at a smaller degree of overall exchange. This suggests that, in *G. mirabilis* A_4-LDH, the population of fast-exchanging amide hydrogens is smaller and that there are fewer residues in the more flexible, rapidly exchanging regions in this form than in the *G. seta* A_4-LDH molecule.

To determine which structures within the A_4-LDH molecule contribute to the difference in H/D exchange seen between the two forms, we used second-derivative analysis to examine the amide I (1600–1700 cm^{-1}) region of the infrared spectra. This method allows separation and narrowing of adjacent bands within the amide I peak. The amide I peak is due mainly to C=O stretching vibrations along the peptide backbone, and within this peak subtle differences in vibration due to the effects of different secondary structures result in bands that can be visualized by second-derivative analysis (Dong et al., 1995; Jackson and Mantsch, 1995). Fig. 5 shows area-normalized, inverted second-derivative amide I spectra of A_4-LDH from *G. mirabilis* and *G. seta* at 20 and 40 °C in 75 % D_2O over the first 60 min of H/D exchange. Because of the area normalization, this analysis does not provide information about the total amount of H/D exchange per unit time. Instead, these data indicate relative levels of exchange within each type of secondary structure.

Examination of these spectra shows that, for each isoform and at each temperature, the major band shifts occur at approximately 1655 cm^{-1} and approximately 1639 cm^{-1} (arrows in Fig. 5). The former has been ascribed to α-helical structure, while the latter corresponds to β-strand (Susi and Byler, 1986). Fig. 6A,B shows the change in height of these peaks over time after exposure to 75 % D_2O. For the β-strand peak at approximately 1639 cm^{-1} (Fig. 6A), there is a clear change in the rate at which H/D exchange occurs as temperature increases from 20 to 40 °C, but there is little difference between the two species at either temperature. This suggests that there are no substantial differences in β-strand conformational flexibility between the two A_4-LDH forms. A different conclusion is reached upon examination of the α-helix peak at approximately 1655 cm^{-1} (Fig. 6B). Here, there is little difference between the species in the rate at which peak height changes at 20 °C or in *G. mirabilis* A_4-LDH at 20 and

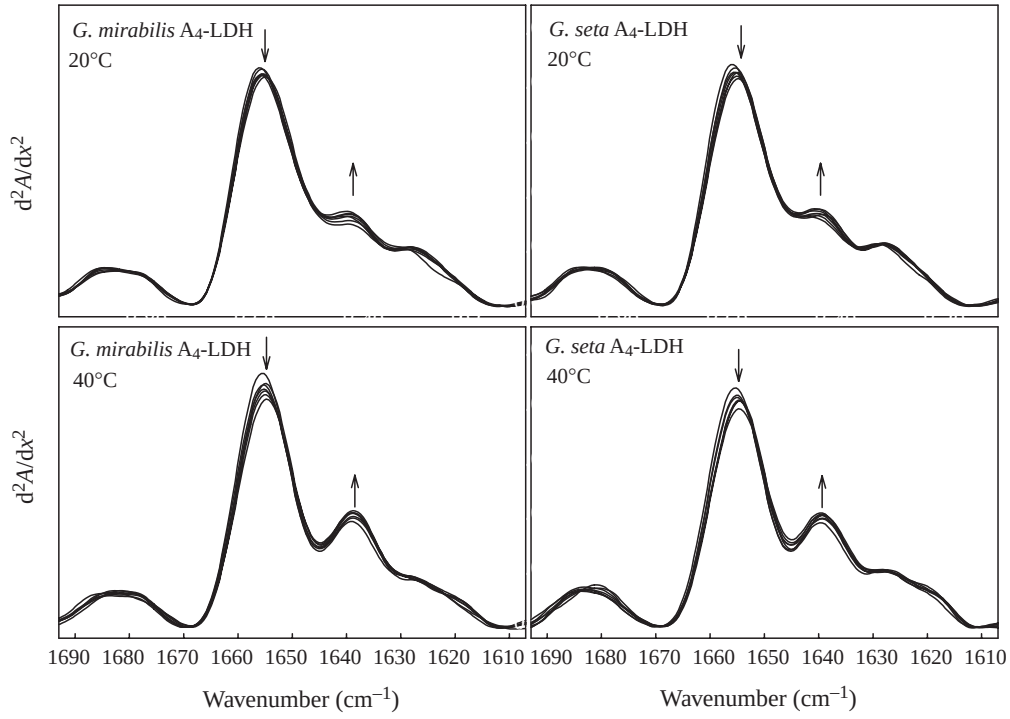

Fig. 5. Inverted second-derivative infrared spectra of muscle-type lactate dehydrogenase (A_4-LDH) across the amide I region. Each panel shows spectra 2, 7, 12, 17, 25, 40 and 60 min after addition of protein to 75 % D_2O buffer. Peaks in the spectra correspond to specific secondary structures, and the arrows at approximately 1655 cm^{-1} (α-helix) and approximately 1639 cm^{-1} (β-sheet) indicate the direction of change in peak height over time. d^2A/dx^2, to be defined.

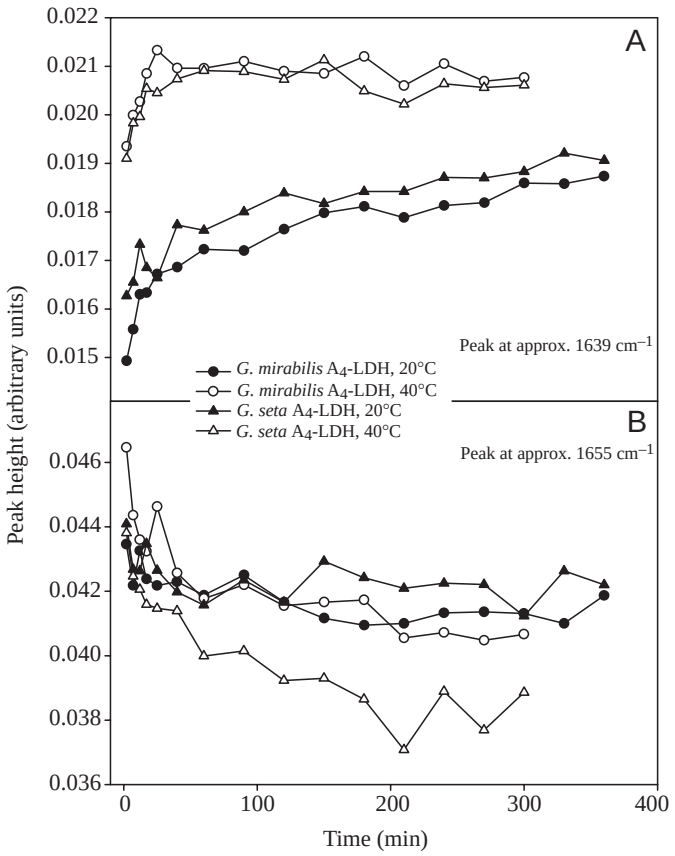

Fig. 6. (A) Change in height of peaks at approximately 1639 cm^{-1} (β-sheet structure) in *Gillichthys* muscle-type lactate dehydrogenases (A_4-LDHs) inverted second-derivative infrared spectra (see Fig. 5) from 2 min to 360 min (20 °C) or 300 min (40 °C) after addition to 75 % D_2O. (B) Change in height of peaks at approximately 1655 cm^{-1} (α-helical structure) over time.

40 °C. The A_4-LDH of *G. seta* measured at 40 °C, however, does show a more rapid change in peak height and, thus, a greater rate of H/D exchange. This indicates that at least part of the difference in conformational flexibility between the *G. seta* and *G. mirabilis* A_4-LDHs must be due to differences in exposure of α-helical structures. Furthermore, because these H/D exchange experiments were relatively short, the α-helices that differ between the two forms must be close to the surface of the protein, where rapid exchange can occur.

Discussion

The function of A_4-LDH from different species, specifically as quantified by its affinity for the substrate pyruvate (K_m^{PYR}), has been shown to correlate with differences in environmental temperature (Fields and Somero, 1998; Coppes and Somero, 1990; Yancey and Somero, 1978). It has been argued that this temperature compensation is adaptive because it maintains substrate affinity within a narrow range, when measured at habitat temperature, across all A_4-LDHs tested (Hochachka and Somero, 2002; Somero, 1995). Such adaptive temperature compensation can occur even when differences in environmental temperatures are relatively small. Holland et al. (1997) showed that differences in habitat temperature of as little as 5 °C were enough to adaptively modify K_m^{PYR} of A_4-LDHs from different species of barracuda (genus *Sphyraena*). These researchers further showed that only one amino acid substitution, out of 331 in the LDH-A monomer, was responsible for the changes in K_m^{PYR} they found. The A_4-LDHs of *G. mirabilis* and *G. seta* have also been shown to differ in substrate affinity (Fields and Somero, 1997) in a manner consistent with adaptation to the different thermal habitats that each species experiences. Here, however, the lack of any difference in primary structure or any obvious post-translational covalent modifications has made determining the structural differences underlying the functional disparities difficult.

Temperature adaptation of protein function appears to rely in large part on the maintenance of an appropriate balance between structural stability, allowing the maintenance of appropriate ligand-binding geometry, and conformational flexibility, allowing catalytic conformational changes to occur without inordinately high energy barriers (Fields, 2001; Feller and Gerday, 1997; Somero, 1995; Jaenicke, 1991). Assuming the validity of this flexibility/stability model of protein adaptation to temperature, and confronted by the lack of differences in the primary structures of the *Gillichthys* A_4-LDHs, we hypothesized that subtly different conformations between the two forms lead to changes in both local and global protein stability and that these differences are manifest in the measured differences in K_m^{PYR}. Although we recognize the possibility that large-scale conformational rearrangements, such as domain swapping, may better explain the apparently high activation energy needed to switch from one conformation to the other (as demonstrated by the absence of interconversion on the time scale of these experiments), we argue that such changes would necessarily bring about larger modifications in K_m^{PYR} than we have measured. Thus, we favor more subtle, local conformational shifts as the likeliest source of differences in the properties of the two orthologs.

Gerstein and Chothia (1990) described the catalytic conformational changes that A_4-LDH undergoes and divided the molecule into a static inner core and a more flexible outer shell of 'major mover' structures whose mobility is important for catalysis. The T_m data we have derived from our Trp fluorescence and CD spectroscopy measurements indicate that the *G. mirabilis* A_4-LDH molecule has a more stable static core: the entire molecule 'melts' at a higher temperature than does the *G. seta* form. In addition, our H/D exchange data show that the flexible outer region of the A_4-LDH molecule is more stable in *G. mirabilis* A_4-LDH at 20 °C than it is in the *G. seta* form, but this difference is lost as temperature is increased to 40 °C.

Interestingly, the greater sensitivity to temperature of *G. mirabilis* A_4-LDH H/D exchange can be correlated with the greater sensitivity of this ortholog's K_m^{PYR} to temperature. We showed previously (Fields and Somero, 1997) that between 10

and 20 °C the K_m^{PYR} values of *G. mirabilis* and *G. seta* A_4-LDHs are similar, but that between 25 and 40 °C the K_m^{PYR} of *G. mirabilis* A_4-LDH rises rapidly while that of *G. seta* A_4-LDH remains relatively constant. Such insensitivity to temperature in the *G. seta* form is a hallmark of eurythermality because it allows A_4-LDH to function optimally across a broad range of temperatures, including those (>30 °C) at which *G. mirabilis* A_4-LDH is losing affinity for substrate. Because *G. seta* lives in an environment with a broader temperature range (5–41 °C) than its congener (9–30 °C), the relative insensitivity to temperature of its A_4-LDH H/D exchange rate (Fig. 4) may be evidence of adaptation to a highly variable thermal environment. In other words, the temperature-insensitivity of both the K_m^{PYR} and the H/D exchange rate of *G. seta* A_4-LDH may arise from the same cause, the relative lack of change in the mobility of the outer shell of the *G. seta* A_4-LDH molecule with temperature. This is plausible because movement of secondary structural elements in this outer shell has been shown to be necessary for catalysis (Dunn et al., 1991; Gerstein and Chothia, 1990).

The results we have reported here allow us to draw inferences regarding where the differences in structure between the orthologs may lie. The far-ultraviolet CD and Trp fluorescence spectroscopy indicate that the secondary and tertiary structures of these A_4-LDH orthologs are very similar. This is not surprising considering the large number of studies of LDH across taxonomic domains, which show that the structure of this enzyme is strongly conserved regardless of environmental temperature or taxonomic affinity (Read et al., 2001; Auerbach et al., 1998), but, combined with the identity in primary structure between the *Gillichthys* A_4-LDHs, it does suggest that the conformational differences between these enzymes must be slight. In addition to the differences in the flexibility of parts of the outer shell between the two A_4-LDH forms discussed above, we have shown that at least one Tyr is in a different microenvironment in the two orthologs, as demonstrated by the different *r* values (Fig. 3B) at 20, 30 and 40 °C. Because it is unlikely that two independent conformational differences are responsible for these two observations, it is parsimonious to assume that the modification in fold or subunit association responsible for the change in hydrophobicity of the Tyr environment is also responsible for changes in flexibility and for the lower T_m and relatively temperature-insensitive K_m^{PYR} of *G. seta* A_4-LDH in comparison with *G. mirabilis* A_4-LDH. These findings, combined with an analysis of the three-dimensional structure of *Gillichthys* A_4-LDH, allow us to identify one region of the A_4-LDH molecule that is likely to be involved in the conformational shift.

To determine the positions of Trp residues in *Gillichthys* A_4-LDH, we examined a homology model of the protein based on dogfish and porcine A_4-LDHs. Fig. 7A shows one LDH-A monomer of the *Gillichthys* A_4-LDH homotetramer. There are five Tyr residues at positions 82, 126, 144, 238 and 246 in the protein sequence. In the context of the static core and mobile outer shell of A_4-LDH (Gerstein and Chothia, 1990), three of the five Tyr residues, Tyr82, Tyr126 and Tyr144, are located in the static core of the molecule. Because these Tyr residues do not move appreciably during catalysis (Gerstein and Chothia, 1990), it is unlikely that they are structurally associated with conformational modifications responsible for differences in K_m^{PYR} and, according to the parsimony argument outlined above, to the other physical differences we have measured between the two A_4-LDHs. Tyr238 is located in the outer shell, on a 'major mover' secondary structural element whose conformational rearrangement is necessary for catalysis (Dunn et al., 1991; Gerstein and Chothia, 1990). This structure, helix α1G–α2G, closes down over the catalytic

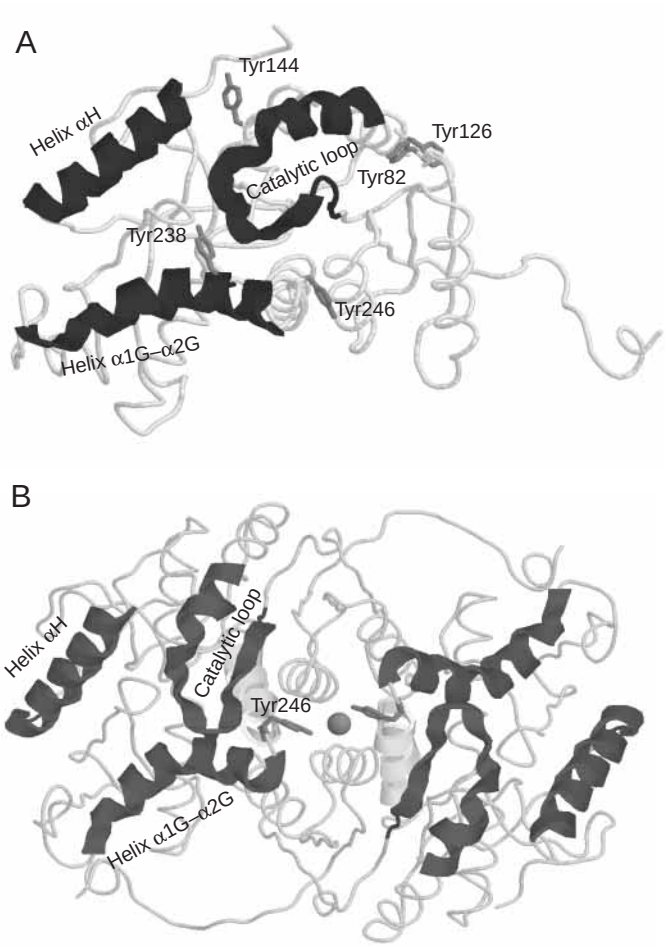

Fig. 7. (A) *Gillichthys* muscle-type lactate dehydrogenase (A_4-LDH) monomer with Tyr residues (gray wire-frame) and 'major mover' (dark gray ribbon) secondary structures labeled. Substrate and cofactor enter the active site through the opening to the left among the major movers, which close down to form the catalytic vacuole. (B) LDH-A dimer, showing major movers, as in A, and the positions of Tyr246 residues hydrogen-bonded to a trapped water molecule (gray sphere) in the intersubunit contact area. Helix α3G is shown as a white ribbon below helix α1G–α2G and Tyr246. Structures were based on the homology model of dogfish A_4-LDH (Abad-Zapatero et al., 1987) and pig A_4-LDH (Dunn et al., 1991) produced using the SWISS-PROT program (Guex and Peitsch, 1997) and visualized using Rasmol.

vacuole after entry of substrate and cofactor (the other major movers, helix αH and the 'catalytic loop,' also close down over the catalytic vacuole from other directions) (Gerstein and Chothia, 1990). Tyr238 is necessarily solvent-exposed; Abad-Zapatero et al. (1987) have argued that rotation of the Tyr238 side chain away from the solvent and into the active site would strongly inhibit enzyme activity. Thus, minor changes in structure should not alter the hydrophobicity of the environment surrounding Tyr238 – it must continue to project into the polar medium for catalysis to occur.

Immediately C-terminal to the mobile helix α1G–α2G is the relatively static helix α3G, which is involved in subunit binding through interactions with helix αC on the complementary monomer (Abad-Zapatero et al., 1987). The final Tyr residue, Tyr246, sits at the junction between helices α1G–α2G and α3G, a 'hinge' between the flexible and static portions of one side of the active site. Tyr246 residues in two monomers hydrogen-bond through a water molecule trapped within the Q-axis interface of the A_4-LDH homotetramer (Abad-Zapatero et al., 1987) (Fig. 7B). Thus, Tyr246 seems to be in an appropriate location to experience changes in hydrophobicity if its microenvironment is altered slightly. That is, if shifts in the interaction between the two subunits were to modify the intersubunit contact region and alter the relative positions of contact residues and trapped water molecules, they would modify the absorbance of Tyr246 in the near-ultraviolet region and be seen as differences in *r* value between the two forms.

In addition, Figs 5 and 6 show that a surface α-helix is involved with differences in H/D exchange rates between *G. mirabilis* and *G. seta* A_4-LDHs. A conformational modification centered around helix α1G–α2G and helix α3G would be consistent with these results and would explain parsimoniously both the difference in *r* and the difference in second-derivative infrared spectra.

Tyr246 can also be associated with changes in K_m^{PYR} between the two *Gillichthys* A_4-LDH molecules. It has been argued that the structural changes underlying changes in enzyme kinetic parameters must be associated with those regions of the molecule that move during catalysis (Fields and Somero, 1998) because it is the energy barriers to conformational change that ultimately control the rates of binding of substrate to and release of product from enzymes, such as A_4-LDH, where the chemical modifications of catalysis are not rate-limiting (Dunn et al., 1991). In the A_4-LDHs of Antarctic notothenioid fishes, helices α1G–α2G and αH (Fig. 7A) were identified as targets of temperature adaptation (Fields and Somero, 1998) because changes in their flexibility would necessarily alter the energy barriers to substrate binding, catalysis and product release. In the notothenioid enzyme, the region N-terminal to helix α1G–α2G was noted as having a number of amino acid substitutions (e.g. Ser→Gly and Thr→Gly) that could lead to greater flexibility in the cold-adapted form. Within the *Gillichthys* A_4-LDHs studied here, Tyr246 sits in the opposite, C-terminal 'hinge' of helix α1G–α2G. Thus, changes in conformation and mobility of this 'major mover' structure, which is closely associated with active site residues (e.g. Thr248), would result in changes in not only *r* or H/D exchange rates but also in substrate affinity.

To summarize, the results obtained using H/D exchange reinforce the argument that α1G–α2G is associated with the conformational and functional differences between the two *Gillichthys* A_4-LDHs. It is the only α-helix near the surface of the protein that both has a nearby buried Tyr and is involved in motions necessary for catalysis. It is only in this area that a minor change in conformation could explain the three differences we have noted between *G. mirabilis* and *G. seta* A_4-LDHs: alterations in K_m^{PYR} (necessarily linked to changes in mobility of the 'major mover' structures), changes in Tyr microenvironment hydrophobicity (i.e. *r* value) and differences in H/D exchange constants associated with α-helical structure.

We therefore identify the region immediately surrounding Tyr246, at the C-terminal end of the α1G–α2G helix, as the area most likely to show conformational differences between the A_4-LDHs of *G. mirabilis* and *G. seta*. We argue that the data we have presented further support the idea that minor changes in the conformation of enzymes, in the absence of any change in amino acid structure, may be a source of adaptive differences in function. The mechanism by which *G. seta* and *G. mirabilis* produce A_4-LDHs with subtly different conformations, either during or after translation, remains to be described.

We would like to acknowledge the support of the NSF, in the form of a grant to G.N.S. (IBN97-27721).

References

Abad-Zapatero, C., Griffith, J. P., Sussman, J. L. and Rossmann, M. G. (1987). Refined crystal-structure of dogfish M_4 apo-lactate dehydrogenase. *J. Mol. Biol.* **198**, 445–467.

Auerbach, G., Ostendorp, R., Prade, L., Korndorfer, I., Dams, T., Huber, R. and Jaenicke, R. (1998). Lactate dehydrogenase from the hyperthermophilic bacterium *Thermotoga maritima*: The crystal structure at 2.1 angstrom resolution reveals strategies for intrinsic protein stabilization. *Structure* **6**, 769–781.

Chazin, W. J., Kördel, J., Drakenberg, T., Thulin, T., Brodin, P., Grundström, T. and Forsén, S. (1989). Proline isomerism leads to multiple folded conformations of calbindin D_{9k}: Direct evidence from two-dimensional ^{1}H NMR spectroscopy. *Proc. Natl. Acad. Sci. USA* **86**, 2195–2198.

Cohen, F. E. and Prusiner, S. B. (1998). Pathologic conformations of prion proteins. *Annu. Rev. Biochem.* **67**, 793–819.

Coppes, Z. L. and Somero, G. N. (1990). Temperature-adaptive differences between the M4 lactate dehydrogenases of stenothermal and eurythermal sciaenid fishes. *J. Exp. Zool.* **254**, 127–131.

Dong, A. and Caughey, W. S. (1994). Infrared methods for study of hemoglobin reactions and structures. *Meth. Enzymol.* **232**, 139–175.

Dong, A., Huang, P. and Caughey, W. S. (1992). Redox-dependent changes in β-extended chain and turn structures of cytochrome-c in water solution determined by 2nd derivative amide I infrared spectra. *Biochemistry* **331**, 182–189.

Dong, A., Matsuura, J., Allison, S. D., Chrisman, E., Manning, M. C. and Carpenter, J. F. (1996). Infrared and circular dichroism spectroscopic characterization of structural differences between beta-lactoglobulin A and B. *Biochemistry* **35**, 1450–1457.

Dong, A., Prestreleski, S. J., Allison, S. D. and Carpenter, J. F. (1995). Infrared spectroscopic studies of lyophilization- and temperature-induced protein aggregation. *J. Pharmac. Sci.* **84**, 415–424.

Dunn, C. R., Wilks, H. M., Halsall, D. J., Atkinson, T., Clarke, A. R.,

Muirhead, H. and Holbrook, J. J. (1991). Design and synthesis of new enzymes based on the lactate dehydrogenase framework. *Phil. Trans. R. Soc. Lond. B* **332**, 177–184.

Feller, G. and Gerday, C. (1997). Psychrophilic enzymes: molecular basis of cold adaptation. *Cell. Mol. Life Sci.* **53**, 830–841.

Fields, P. A. (2001). Protein function at thermal extremes: balancing stability and flexibility. *Comp. Biochem. Physiol.* **129A**, 417–431.

Fields, P. A. and Somero, G. N. (1997). Amino acid sequence differences cannot fully explain interspecific variation in thermal sensitivities of gobiid fish A_4-lactate dehydrogenases (A_4-LDHS). *J. Exp. Biol.* **200**, 1839–1850.

Fields, P. A. and Somero, G. N. (1998). Hot spots in cold adaptation: Localized increases in conformational flexibility in lactate dehydrogenase A_4 orthologs of Antarctic notothenioid fishes. *Proc. Natl. Acad. Sci. USA* **95**, 11476–11481.

Gerstein, M. and Chothia, C. (1991). Analysis of protein loop closure: two types of hinges produce one motion in lactate dehydrogenase. *J. Mol. Biol.* **220**, 133–149.

Gregory, R. B. (1983). Comparison of analytically and numerically derived hydrogen exchange-rate distribution functions. *Biopolymers* **22**, 895–909.

Guex, N. and Peitsch, M. C. (1997). SWISS-MODEL and the Swiss-PdbViewer: An environment for comparative protein modelling. *Electrophoresis* **18**, 2714–2723.

Hochachka, P. W. and Somero, G. N. (2002). *Biochemical Adaptation*: *Mechanism and Process in Physiological Evolution*. Oxford: Oxford University Press.

Holland, L. Z., McFall-Ngai, M. and Somero, G. N. (1997). Evolution of lactate dehydrogenase-A homologs of barracuda fishes (genus *Sphyraena*) from different thermal environments: Differences in kinetic properties and thermal stability are due to amino acid substitutions outside the active site. *Biochemistry* **36**, 3207–3215.

Hvidt, A. and Nielsen, S. O. (1966). Hydrogen exchange in proteins. *Adv. Protein Chem.* **21**, 287–386.

Jackson, M. and Mantsch, H. H. (1995). The use and misuse of FTIR spectroscopy in the determination of protein structure. *Crit. Rev. Biochem. Mol. Biol.* **30**, 95–120.

Jacobson, K. B., Murphy, J. B. and Hatman, F. C. (1970). Isoenzymes of *Drosophila* alcohol dehydrogenase. I. Isolation and interconversion of different forms. *J. Biol. Chem.* **245**, 1075–1083.

Jaenicke, R. (1991). Protein stability and molecular adaptation to extreme conditions. *Eur. J. Biochem.* **202**, 715–728.

Kendrick, B. S., Chang, B. S., Arakawa, T., Peterson, B., Randolph, T. W., Manning, M. C. and Carpenter, J. F. (1997). Preferential exclusion of sucrose from recombinant interleukin-1 receptor agonist: Role in restricted conformational mobility and compaction of the native state. *Proc. Natl. Acad. Sci. USA* **94**, 11917–11922.

Kendrick, B. S., Dong, A., Allison, S. D., Manning, M. C. and Carpenter, J. F. (1996). Quantitation of the area of overlap between second-derivative amide I infrared spectra to determine the structural similarity of a protein in different states. *J. Pharmac. Sci.* **85**, 155–158.

Kim, Y. S., Wall, J. S., Meyer, J., Murphy, C., Randolph, T. W., Manning, M. C., Solomon, A. and Carpenter, J. F. (2000). Thermodynamic modulation of light chain amyloid fibril formation. *J. Biol. Chem.* **275**, 1570–1574.

Marangos, P. J. and Constantides, S. M. (1974). Multiple forms of flounder muscle glyceraldehyde 3-phosphate dehydrogenase: subunit composition, properties and tissue distribution of the forms. *J. Biol. Chem.* **249**, 951–958.

Miller, D. J. and Lea, R. N. (1972). Guide to the coastal marine fishes of California. *Cal. Fish Bull.* **157**.

Miller, D. W. and Dill, K. A. (1995). A statistical mechanical model for hydrogen exchange in globular proteins. *Protein Sci.* **4**, 1860–1873.

Ozernyuk, O. D., Klyachko, O. S. and Polosukhina, E. S. (1994). Acclimation temperature affects the functional and structural properties of lactate dehydrogenase from fish (*Misgurnus fossilis*) skeletal muscles. *Comp. Biochem. Physiol.* **107B**, 141–145.

Pace, C. N. (1986). Determination and analysis of urea and guanidine hydrochloride denaturation curves. *Meth. Enzymol.* **131**, 266–280.

Patino, M. M., Liu, J. J., Glover, J. R. and Lindquist, S. (1996). Support for the prion hypothesis for inheritance of a phenotypic trait in yeast. *Science* **273**, 622–626.

Ragone, R., Colonna, G., Balestrieri, C., Servillo, L. and Irace, G. (1984). Determination of tyrosine exposure in proteins by 2nd derivative spectroscopy. *Biochemistry* **23**, 1871–1875.

Read, J. A., Winter, V. J., Eszes, C. M., Sessions, R. B. and Brady, R. L. (2001). Structural basis for altered activity of M- and H-isozyme forms of human lactate dehydrogenase. *Proteins: Struct. Funct. Genet.* **43**, 175–185.

Servillo, L., Colonna, G., Balestrieri, C., Ragone, R. and Irace, G. (1982). Simultaneous determination of tyrosine and tryptophan residues in proteins by 2nd derivative spectroscopy. *Anal. Biochem.* **126**, 251–257.

Somero, G. N. (1969). Pyruvate kinase variants of the Alaskan King crab: Evidence for a temperature-dependent interconversion between two forms having distinct and adaptive kinetic properties. *Biochem. J.* **114**, 237–241.

Somero, G. N. (1995). Proteins and temperature. *Annu. Rev. Physiol.* **57**, 43–68.

Susi, H. and Byler, D. M. (1986). Resolution-enhanced Fourier transform infrared-spectroscopy of enzymes. *Meth. Enzymol.* **130**, 290–311.

Xue, Q. and Yeung, E. S. (1995). Differences in the chemical reactivity of individual molecules of an enzyme. *Nature* **373**, 681–683.

Yancey, P. H. and Somero, G. N. (1978). Temperature dependence of intracellular pH: Its role in conservation of pyruvate apparent K_m values of vertebrate lactate dehydrogenases. *J. Comp. Physiol.* **125**, 129–134.

Zhang, H. J., Sheng, X. R., Niu, W. D., Pan, X. M. and Zhou, J. M. (1998). Evidence for at least two native forms of rabbit muscle adenylate kinase in equilibrium in aqueous solution. *J. Biol. Chem.* **273**, 7448–7456.